ULTRASONIC AND ACOUSTIC MICROMECHANICAL DEVICES

Ultrasonic and acoustic devices are sensors and actuators for mechanical pressure waves with acoustic (10 Hz to 15 kHz) and ultrasonic (>15 kHz) frequencies. The devices can be classified into two categories. First, many devices process pressure waves where sound and ultrasound are the final desired entity. Examples are microphones, loudspeakers, sonar receivers, and medical imaging systems. Second, there are devices that utilize vibratory energy in sound and ultrasound waves to cause a secondary desired effect. Examples of this type of devices are acoustic chemical sensors, ultrasonic motors, microfluidic pumps, ultrasonic surgical tools, ultrasonic bonders, ultrasonic atomizers, and acousto-optic modulators.

A further classification of acoustic devices is made between high-intensity (>1 W/cm^2) and low-intensity devices (<1 W/cm^2). Low-intensity applications include microphones, chemical sensors, and sonar receivers. The high-intensity applications include motors, pumps, bonders, surgical tools, etc. Table 1 distributes the sonic applications among the four different categories possible. The reader is referred to Ref. 1 for

Table 1. Classification of Ultrasonic Applications

	Direct Use of Sonic Energy	Indirect Use of Sonic Energy
Low intensity	Microphones, sonar receiver	Chemical sensors, acousto-optic modulation
High intensity	Loudspeakers, sonar generator	Microfluidic pumps, surgery, atomization, bonding, cutting

J. Webster (ed.), *Wiley Encyclopedia of Electrical and Electronics Engineering*.

a more complete discussion on applications of acoustic and ultrasound devices.

CHARACTERISTICS OF MEMS ACOUSTIC DEVICES

Several features distinguish micromachined acoustic systems made by MEMS (microelectromechanical system) techniques from those fabricated by traditional means. Listed below are the features of micromachining and how they affect the characteristics of acoustic devices:

1. *Integration of Electronics and Mechanical Components.* In common with all acoustic devices is the mechanical movement of the active element, and in most devices the mechanical displacement is actuated or sensed electronically. MEMS technology allows a natural integration of electronic and mechanical components, which results in substantial advantages over conventional acoustic and ultrasonic devices. In acoustic sensing applications (e.g., microphones), the *signal-to-noise* ratio is a function of the mechanical sensor element, the electronics, and their electrical interconnects. Electrical noise in electrical interconnects can be minimized by placing a preamplifier as close as possible to the sensing element. MEMS technology allows the placement of the electronics very close to the sensing elements in order to reduce the parasitic capacitance of the interconnects. However, processing incompatibilities may make it difficult to fabricate the mechanical and electrical elements simultaneously, as lower yields and higher costs may result. Two attractive solutions are to post-process mechanical elements onto CMOS dies (4) and to assemble automatically previously fabricated micromechanical and electronic elements (4).
2. *Small Devices.* MEMS technology allows the fabrication of extremely small mechanical parts, accurately, and in a repeatable way. For example, cantilevers measuring 10 μm × 10 μm × 2 μm can be made using surface micromachining (see below). Integration of active electronics further allows devices that are very small. The size reduction has three effects on acoustic devices. First, *large arrays* of devices can be fabricated in the same space where conventional machining allowed only one device to be built. Second, the extra available space can be used to integrate more devices and therefore add functionality to the entire system. Third, the extremely small size allows the possibility of system size reduction. For example, micromachining allows the direct surgical placement of micromachined microphones and loudspeakers inside the ear for superior hearing aid. The very small size results in very lightweight, inconspicuous structures, and generally reduces the energy needed to power them.
3. *Unique Material Properties of Silicon.* Silicon is the most common material encountered in micromachined acoustic devices. Its material properties make it ideal for ultrasonic and acoustic devices. Other materials that are commonly used in micromachining are silicon nitride, polysilicon, and silicon dioxide. Their material properties relevant to acoustics are listed in Table 2. Thin film piezoelectric materials are also critical to micromachined acoustic devices, and they will be discussed later in this chapter.
   a. *Density.* The density of silicon is 2330 kg/cm^3, a value that is one-half to one-third that of metals. This property further enhances the lightweight feature of devices.
   b. *High Speed of Sound.* In acoustics and ultrasonics, given a frequency of operation, the speed of sound determines the wavelength of the pressure waves. The speed of sound in silicon is 9000 m/s, a value about twice the speed of sound in metals, increasing the wavelength for a given operating frequency. This property allows the fabrication of devices that are larger and easier to package.
   c. *Low Acoustic Attenuation.* The acoustic loss of materials results from dislocations driven by pressure waves in solids. There are negligible volume dislocations (~1/cm^3) in commercially available prime-grade silicon wafers. Therefore the bulk losses for acoustic and ultrasonic waves are almost negligible. In fact, the measured internal quality factor of silicon exceeds 10^6 (2). The acoustic losses in silicon are typically an order of magnitude lower than in metals. This results in micromachined devices that have higher quality factors. This fact affects device performance in many positive ways. Low internal loss in sensing devices such as microphones leads to *higher*

Table 2. Relevant Properties of Various Materials

	Property							
Material	Y GPa	Strength GPa	Density kg/m^3	S_mc m/s	Hardness kg/mm^2	Toughness MPa · m$^{1/2}$	Acoustic Loss $1/Q$	Thermal Conductance (W/m)K^{-1}
Silicon	190	7	2300	335	850	1	$\sim 10^{-5}$	130
Diamond	1035	53	3500	881	7000	2.5	$\sim 10^{-5}$	600
Si_3N_4	385	14	3100	405	3486	5	$\sim 10^{-5}$	10–20
SiO_2	73	8.4	2500	622	820	0.6	$\sim 10^{-5}$	1–2
SiC	700	21	3200	444	2480	4	$\sim 10^{-5}$	70–80
Titanium (C-120-AV)	110	0.9	4430	41	390	50	$\sim 3 \times 10^{-4}$	7–10
Carbon steel	200	2.1	7900	53	660	100	$\sim 10^{-4}$	60–70
PZT-4	85	0.024	7600	0.93	—	—	2.5×10^{-3}	—
PZT-6H	68	0.028	7700	1.21	—	—	1.54×10^{-2}	—

sensitivities. Loss mechanisms in solids tend to disperse energy and create noise. Therefore low acoustic loss leads to *lower noise* levels. Losses in materials also means that some of the energy is lost as heat. If these can be minimized, then devices have *lower power requirements,* and *less heat generation.* For high-intensity devices, having lower heat generation is of particular importance. Generally, high-intensity acoustic devices are in contact with some other material to be processed ultrasonically. The contact at high velocities results in high frictional losses at the transducer/material interface. The friction results in large heat generation and heat-induced transducer damage.

d. *High Thermal Conductivity.* The thermal conductivity in silicon is an order of magnitude larger than in metals. Even if heat is generated, it can be carried away to a heat sink more readily than in metals.

e. *High* $S_m c$. The maximum velocity at which an acoustic or ultrasonic device can be driven is proportional to $S_m c$, where S_m is the yield or fracture strain, and c is the speed of sound. This product for silicon that has a thermal oxide coating is 335 m/s. The $S_m c$ for the highest strength metal is 45 m/s, or about eight times smaller. Hence silicon devices can be driven to much *higher particle velocities* than metal devices. In most ultrasonic applications where the pressure waves cause a physical change in the material being processed, the process throughput is quadratically related to the ultrasonic particle velocity in the medium. A factor of eight increase in the particle velocity should cause a 64 times increase in process throughput (3).

f. *Lack of Fatigue.* Fatigue in materials results from dislocation movements and dislocation accumulation in such a way that the strength in the high strain areas is decreased over time and the device can fail catastrophically. The frequency ranges of commercial metal high-intensity actuators are limited by fatigue. Since there are very few dislocations in silicon and low dislocation mobilities in other micromachining materials such as silicon nitride, silicon dioxide, and polysilicon, very little fatigue degradation of material properties is encountered. Hence silicon-based micromachined devices can operate at *higher frequencies* for longer periods without fatigue failure. This property will enable silicon micromachined acoustic sensors to be used in applications requiring long-term stable use. Such applications include sensors and actuators in space, underground, and in implantable devices.

MEMS FABRICATION TECHNIQUES

The definition of “micromachine” is not unique and changes from person to person. Micromachining is a rapidly evolving area of research, whose definition is still changing. The definition that at least one dimension of a micromachine be in the submicron to a few micron range is generally accepted without too much argument. For a more detailed treatment of micromachining techniques, see Ref. 4.

Because more tools are continually being developed for micromachining, it is impossible to summarize micromachining in a complete and an all-encompassing manner. Hence, in this article the focus will be on micromachining principles that are common to most micromachine fabrication. Our main interest is with silicon bulk and surface micromachining techniques that have resulted in research and commercial devices.

Anisotropic Etching

Silicon atoms in a silicon crystal are arranged in the zincblende structure. Entire silicon crystals can be formed by simple repetition of the basic unit cell. Each of the faces of the unit cell can be described by a vector such as ⟨100⟩, ⟨111⟩, ⟨110⟩, and so on. One can buy silicon wafers whose surface consists of unit cells with the same face exposed. Commercial wafers come in two orientations, ⟨100⟩ or ⟨110⟩. The ⟨110⟩ wafers have traditionally been used for the bipolar circuit process, but the ⟨100⟩ wafers which are used in MOS-like processes lead to a better gate oxide. Industry standards in the form of wafer cuts were developed to easily distinguish the different kinds of wafers. The reader is referred to Ref. 4 for more details on commercial wafers.

Anisotropic etching is based on the wide variation in etching rates as a function of the exposed crystal planes. It is readily observed that the ⟨111⟩ direction has the lowest etching rate and that ⟨100⟩ has the highest etch rate. The origin of the anisotropic etch rates is still under investigation. The leading theories are based on the fact that the silicon atom densities vary considerably over different crystal planes.

Anisotropic etching is performed by typically coating the wafer with a masking layer that does not etch appreciably in the etchant. In general, special jigs are used to align the mask to an orienting surface ground on the edge of the wafer so that etching occurs with respect to a certain crystal direction. The most common form of anisotropic etching is performed on ⟨100⟩ wafers. The ⟨111⟩ planes act as etch stops. The ⟨111⟩ crystal planes are oriented at 54.74° to the wafer surface, and a wall with that angle results as shown in Fig. 1. If one uses ⟨110⟩ wafers, one can achieve vertical walls. In the ⟨100⟩ wafers the surface etches at typical etch rates of 1 μm/min, while the ⟨111⟩ planes, which are at a 54.74° angle, etch at roughly 0.1 nm/min. A typical mask layer of silicon dioxide etches at roughly 0.001 μm/min. The etch-rate-ratio between the silicon and oxide is 1000 : 1 and results in the capability

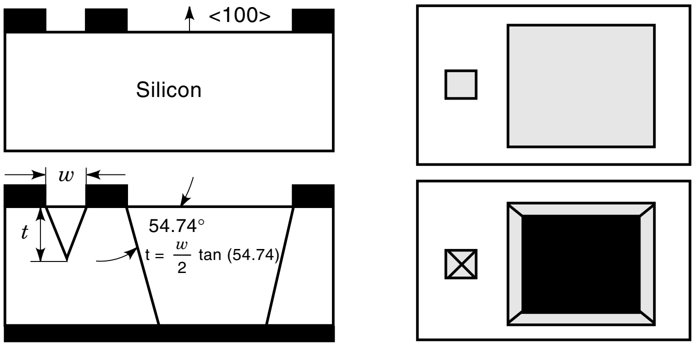

Figure 1. Bottom shows resulting self-terminated pyramid and through-wafer etched cavity as a result of mask in top with a ⟨100⟩ silicon wafer. Right side shows top view of wafer.

to etch through a silicon wafer. Hence, two etch ratios are important. One is the ratio between the ⟨100⟩ and the ⟨111⟩ etch rates, also known as the anisotropy ratio. The second is the ratio of the silicon etch rate to the mask etch rate, called the mask-etch-rate ratio.

Masking Layers. Typical masking layers on silicon are thermal (dry or wet) oxide, and low-stress silicon nitride thin films. Silicon dioxide etch rates are usually higher than silicon nitride etch rates. However, since oxides are more commonly available from ubiquitous thermal oxidation furnaces, it is preferred to silicon nitride, which can be deposited only in the less common LPCVD (low pressure chemical vapor deposition) furnaces. Low-temperature plasma deposition of either oxide or nitride films results in pinhole-contaminated films. Evaporated, sputtered, or electroplated metal thin films can also be used as masking layers with selected anisotropic etchants, as described below.

Anisotropic Etchants. Many anisotropic etchants have been identified over the last 30 years. The factors affecting the etchant choice are the desired etch-rate (determines the time of etch), masking material and its etch rate, temperature required, and chemical toxicity. The etchants fall under two broad categories of organic and inorganic alkaline solutions.

EDP (ethylene-diamene-pyrocatechol) is the most common organic etchant used. This is a highly toxic combination of carcinogenic, irritant, and pyrolytic chemicals, which micromachinists have used for decades under the protection of hoods, protective clothing, and masks. Furthermore, these solutions age, requiring constant reformulation. EDP based solutions have the main advantage of very low metal (Ag, Au, Cr, Cu, Ta) etch rates, making possible the use of metals as masks for anisotropic etching. EDP's low silicon dioxide etch rate allows one to do through-wafer etching with very thin oxide coatings.

TMAHW (tetramethyl ammonium hydroxide water) organic etch solutions are more IC compatible because the solution does not decompose at temperatures below 130°C. They have a much lower oxide etch rate than does KOH (potassium hydroxide), which is discussed below. At high pH values, TMAH solutions etch aluminum at only 0.01 μm/min. Hence it is possible to use aluminum as a masking material with TMAH. The disadvantage with TMAH is the low anisotropy ratio (12 to 50) as compared with that of KOH (500 to 1000). Hence, considerable underetching can occur with TMAH.

Alkaline Etches. The most common alkaline etch is a KOH/water solution used at 80°C to 90°C. Typically the KOH concentration is varied from 20% to 60%. Concentration and the temperature affect the etch rates, etch-rate-ratio, and the etched surface roughness. Higher KOH concentrations result in lower etch rates and smoother surfaces.

One can calculate the mask thickness required for a given depth of silicon etching using measured etch rate data. For example, to do through-wafer etching with an oxide mask, at 90°C to achieve 2 μm/min, it can be shown that 3 μm of oxide are required. This oxide thickness is nearly impossible to achieve in reasonable processing times by standard wet oxidation. Hence, silicon nitride films are more commonly used with KOH etching solutions.

In addition to the micro roughness, KOH etching results in a bowing effect at the intersection of the ⟨100⟩ and the ⟨111⟩ planes. This is believed to occur due to the presence of excess ionic reactive species available near the edges where ⟨111⟩ planes do not consume the ions at all. Stirring the solution can reduce such nonuniformity. Stirring is also used to remove adhering reaction product gas bubbles from the silicon surface. Addition of isopropyl alcohol to the etch bath results in smoother etch surfaces. Lower-density alcohol rises to the top of the bath and helps to regulate the temperature inside the etch bath. Metals can be added to the etching bath to increase etch rates (5).

A disadvantage of KOH and other alkaline solutions is that they can cause blindness by direct contact. Another disadvantage of KOH is that the potassium ions diffuse into silicon as an impurity and hence KOH is not considered IC-compatible.

Effect of Doping on Etching Rates

Highly doped *p*-type (concentration $>10^{21}\,\text{cm}^{-3}$) areas of silicon behave as etch stops in the alkaline anisotropic etchants. This agrees well with the electrochemical model of the anisotropic etching behavior, in which the excess holes in the p^{++}-doped silicon can pin the fermi level much lower than the redox potential in the etching bath, eliminating the charge exchange and the resulting chemical reaction (5). Cantilevers and beams of p^{++}-doped areas have been readily made using this process (Fig. 2). The thickness of the doped region is usually limited to 2 μm to 3 μm because of diffusion-limited growth of doped regions. However, workers at the University of Michigan have developed an extended time diffusion doping process that allows for doping to 10 to 20 μm depths.

Porous Silicon Formation

Porous silicon is a term for uniformly etched silicon with pores having diameters ranging from nanometers to micrometers, and lengths up to millimeters. Hence, extremely high-aspect ratio devices are possible. Porous silicon can be fabricated by electrochemically etching silicon in a hydrofluoric acid solution. The silicon oxidizes and then is etched by the HF acid. The pore size can be controlled by HF concentration or exposure to electron–hole generating photonic sources. Although etching a planar surface produces randomly distributed pores, a surface with pore-initiating features can result in highly organized pores.

MEMS Prototype Structures

By anisotropic etching, one can generate prototypical structures that are the foundation of most micromechanical systems. One of the common structures is the thin diaphragm (membrane). The membrane can be formed by many methods, as shown in Fig. 2. One method, Fig. 2(a) and (b), is to time-etch the silicon if the etch rate is known with confidence. However, etch rates vary considerably as the solution concentration and/or temperature changes. Hence, the membrane thickness reproducibility is not better than 5 μm to 10 μm. But a trick can be used to better reproduce membrane thickness, as shown in Fig. 2(c). Early in the etching process, a top window in the masking layer terminates in a pyramid. The mask opening can be adjusted so that the pyramid height cor-

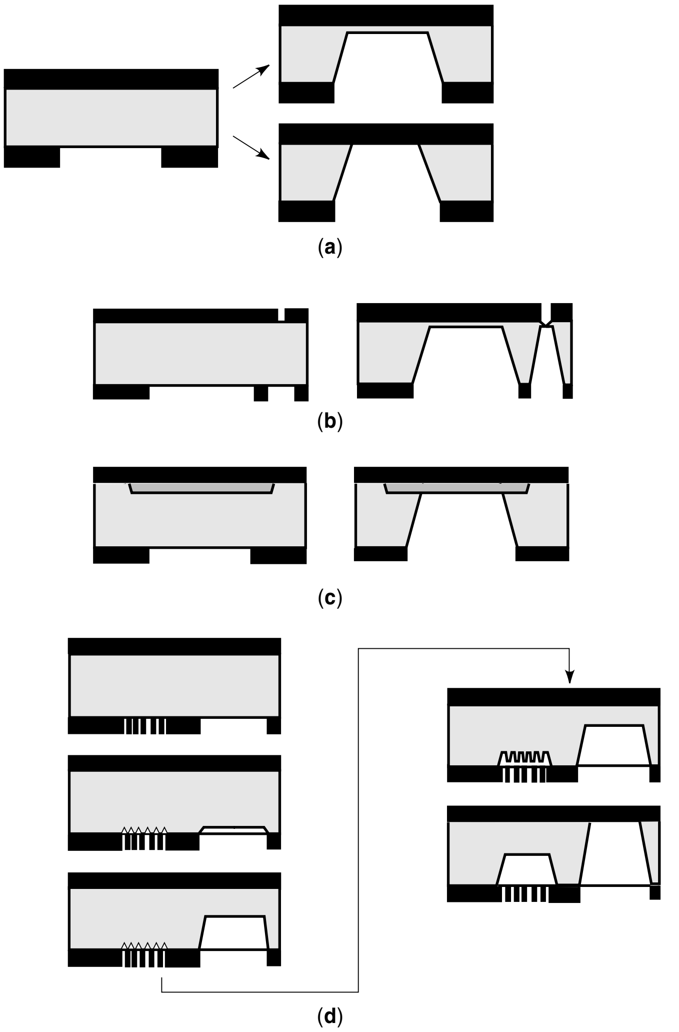

Figure 2. Some techniques to produce membranes and plates anchored by silicon substrate. (a) Timed etch produces silicon plates or etching to mask film produces thin-film membrane. (b) A self-terminating pyramid from top is used to stop etch when an optic signal is transmitted from the bottom. (c) Etch stops such as p^+-doped silicon or electrochemically active layers can be used to stop etch. (d) The grill technique to obtain different height cavities with one mask.

responds to the desired plate thickness. As the etch front from the bottom approaches the pyramid tip, a predetermined amount of light transmission through the etch front and the pyramid surface is used as an indicator to stop the etching. This technique will result in membranes whose thickness varies by only 2 μm to 3 μm from wafer to wafer.

As shown in Fig. 2(d), thin membranes can also be obtained by using membrane materials that act as etch stops for the etching electrolyte. Etching through the wafer forms silicon nitride or silicon dioxide membranes. Highly p^{++}-doped silicon then acts as the etch stop, and the result is a p^{++}-doped silicon membrane.

By electrically biasing doped silicon sections, one can electrically control population of charge carriers at the semiconductor-electrolyte interface. The ability to control the carriers can be used to modulate the electrochemical reaction. Typically a *p*–*n* junction is reverse biased. The voltage drop is largely across the *p*–*n* diode, leaving the *p*-type silicon surface at open-circuit potential. The KOH etches the *p*-type silicon until it encounters the *n*-type silicon. The *p*–*n* junction is destroyed, and the *n*-type silicon gets biased to eliminate any carriers on the surface. This stops the etching completely (6). An effective electrochemical reverse-biased diode stops the moving etch front near the diode depletion region. Such techniques can be used to control diaphragm thicknesses to within nanometers. In addition to electrical biasing, one can bias silicon by generating electrons and holes via photonic illumination. Hence, for repeatable membrane thicknesses, one has to etch in the dark.

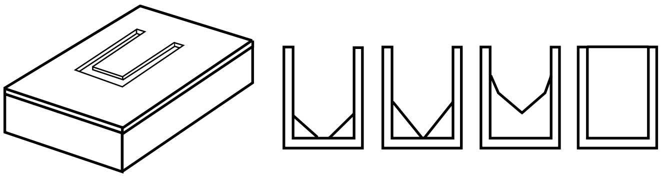

Figure 3. The masking layer is underetched at the concave corners, until the etch front reaches the ⟨111⟩ planes at the cantilever neck.

Besides membranes, cantilevers can be made of silicon or etch stop materials by similar techniques. Figure 3 shows a cantilever of silicon nitride formed by exposing the silicon from the front side of the wafer. Similar techniques can be used to form a p^{++}-doped cantilever, as shown in Fig. 4.

Plasma and Vapor Phase Etching ("Dry Etching")

Dry etching can be classified into plasma and vapor phase etching. Plasma etching is used in micromachining for many reasons, the most important being the possibility of achieving vertical etch sidewalls. In plasma etching the reactive gas is mixed with a dilutant gas and exposed to high-energy radiofrequency electric fields. These fields ionize the gas molecules, creating electrons that further ionize the gas and lead to a stable mix of ions and electrons. For plasma etching, the reactive ions have to diffuse toward the surface, diffuse on the surface, react with the surface atoms, and then diffuse away into the plasma. If the ions are very energetic, pure physical etching will occur by ion-surface momentum transfer during impacts. The pressure, temperature, and RF power of the plasma influence the etch rates, etch uniformity, and etch profiles.

Plasma Etching. Silicon is commonly etched in a fluorine plasma, which consists of SF_6 or CF_4 gases mixed with oxygen

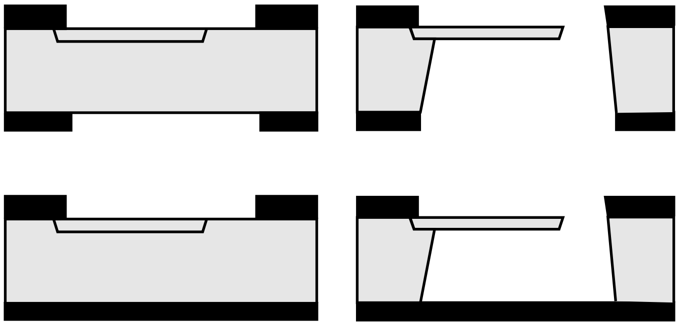

Figure 4. Methods of creating cantilevers by underetching.

in the plasma. These gases directly react with the silicon atoms and form polymers which are etched by dilutant oxygen radicals. Usually the plasma density is low, and the reaction rate is very high, causing a reaction-rate limited etching. The supply-limited reaction results in a loading effect whereby the more exposed areas of silicon are etched more slowly than the less exposed areas.

Chlorine is not as reactive as fluorine with silicon. Hence chlorine-silicon plasma-assisted reaction has to be catalyzed by high-energy ion bombardment. In a low-density plasma the momentum from the ions is transferred more favorably to the bottom surface of the etch front than to the sidewalls. This phenomenon can result in vertical sidewalls. In particular, polymers can be formed on the sidewalls treated with photoresist and/or carbon polymerization. Asymmetric momentum transfer from oxygen radicals again would lead to sidewall passivation. Since low reaction rates also result in a smaller loading effect, when a degree of anisotropy is required, one can use chlorine radicals by employing gases such as $SiCl_4$, CCl_4, BCl_3, and Cl_2.

Vapor Phase Etching of Silicon. Silicon etching due to XeF_2 vapor has been known since the 1960s. However, recently it was rediscovered in the micromachining context. When gently heated, solid XeF_2 sublimes. The XeF_2 vapor instantaneously decomposes on a silicon surface, and the fluorine reacts with the silicon atoms. The XeF_2 silicon etch is isotropic. In particular, XeF_2 is highly selective to silicon; it does not etch photoresist, metals, or silicon dioxide. To get smooth XeF_2 etches, any residual silicon dioxide, which can act as an etch stop, needs to be removed in HF. Polysilicon can be prevented from etching in XeF_2 by oxidizing it slightly, simply by letting it sit in air for two days. The use of XeF_2 etching has been shown to be advantageous for creating microstructures by postprocessing on standard CMOS wafers.

Silicon Bonding

The need to bond silicon to other materials or silicon itself came from packaging requirements. Glass–silicon bonding was developed to cover silicon micromachined devices with a glass cap.

Anodic Bonding. Glass-silicon bonding originated from metal-to-glass "Mallory" bonding. The glass wafer is placed on top of the silicon wafer in a vacuum environment to eliminate trapped air at the glass–silicon surface. A high electric field ($\sim 7 \times 10^6$ V/m) is established across the glass–silicon sandwich at elevated temperatures (350°C to 400°C). The trapped ions (typically glass is sodium and potassium rich) in the glass migrate toward the interface under the influence of the electric field and the increased ionic mobility at high temperatures. Counteracting mirror charges develop in the silicon, producing a strong electric field at the interface. When the silicon–glass sandwich is brought back to room temperature and the electric field removed, the ions are trapped at the interface. If the glass and the silicon have different thermal expansion coefficients, the resulting interfacial thermal stresses can cause deformation of the sandwich at room temperature. Hence, much early work was devoted to finding glasses with the same net thermal expansion as silicon at the bonding temperature. One such glass is the Corning 7740 (Pyrex). The electrostatic field must be high enough to permanently bond the two materials. When the field strength is very high, the bonding process is forgiving to surface irregularities and contamination.

Low-Temperature Glass Bonding. The procedure of applying high electric fields can be eliminated by the use of very thin films of glass that are deposited using microfabrication techniques or bought from commercial glass frit companies. Thin films of phosphoslicate or borosilicate glass can be sputtered or spun on. The substrate to be bonded is placed on the glass under pressure and at an elevated temperature. In general, the bond strengths obtained are not as high as those obtained with fusion or anodic bonding.

Reactive Metal Bonding. In reactive metal bonding, one utilizes the fact that positive free energy is associated with the chemical reaction of a metal with silicon. When the metal and silicon are put together, the combination melts at a lower temperature than either metal or silicon alone. For example, gold reacts with silicon at low temperatures (363°C) to form a Si–Au eutectic. Typically gold is evaporated, sputtered, or electroplated onto the surface to be bonded to a silicon surface. When these areas are put in contact under vacuum and at the eutectic temperature, the metal diffuses into the silicon, forming the eutectic melt. When the interface is cooled, the melt solidifies, forming the bond layer. One has to prepare the silicon surface carefully to eliminate any diffusion barriers, such as silicon dioxide.

Surface Micromachining

A sacrificial layer material is deposited first on a silicon wafer, coated with a passivation layer such as silicon nitride. Lithography is used to define areas where the sacrificial etch is removed selectively (Fig. 5). A conformal thin film of the structural material, such as polysilicon, is deposited over the entire wafer. The structural layer is patterned using lithography and chemical or plasma etching, which is terminated on

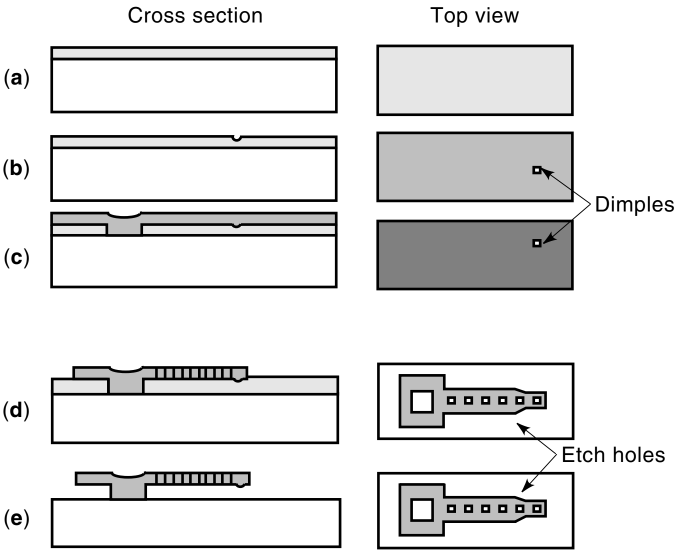

Figure 5. The basic surface micromachining process used to fabricate surface micromachined structures.

the sacrificial layer by a timed etch or by selective etching chemistry. Then the entire sacrificial layer, but not the structure material, is etched selectively. The etch-rate ratio of the sacrificial film relative to that of the structure has to be very high in order to maintain structural layer thickness. Furthermore, the interfacial stresses between the sacrificial and the structure layer, and the internal stresses of the structural layer, have to be very low to avoid curling of the structural material after the release step. The structure material also has to be nearly defect free to reduce the surface roughness that typically results from the sacrificial layer etch. There are very few combinations of sacrificial/structural materials that meet all these conditions.

Nathanson at Westinghouse made surface micromachines as early as 1965. He used aluminum as the structure material and silicon dioxide as the sacrificial material. The somewhat unpredictable and weak material properties of aluminum eventually made this technology an interesting curiosity. Roger Howe at Berkeley and Henry Guckel at the University of Wisconsin in the early 1980s developed an LPCVD polysilicon process for making stress-free polysilicon films on silicon dioxide. They were able to make bridges and cantilevers by using the polysilicon as the structural material. Howe demonstrated vapor sensors that utilized the resonance frequencies of the mechanical structures. Once stress-free films of polysilicon had been made, people began to make a wide variety of surface-micromachined structures.

Polysilicon/PSG Surface Micromachining. Polysilicon and PSG (phosphosilicate glass–phosphorus-doped silicon oxide) are the most popular structural and sacrificial materials, respectively. LPCVD PSG films are chosen for their much higher etch rates in hydrofluoric acid compared to those of thermal or wet oxides. The PSG is deposited typically in gases at low pressures and temperatures. It is patterned using lithography and a dry plasma etch to obtain vertical side walls. Polysilicon is deposited in an LPCVD tube with $SiCl_4$ as the source gas with nitrogen and hydrogen as dilutants. Appropriate pressure and temperature result in reasonable deposition rates. Subsequently, a high-temperature anneal step is performed to densify the PSG glass and diffuse phosphorus into the undoped polysilicon. The densification helps to reduce the interfacial and internal stresses. The polysilicon is patterned and etched in a plasma etch. Various wet etches have been tried, each producing different final structures. Concentrated HF solutions give very fast etch rates along with high surface roughness. Dilute HF gives a slower etch rate but does not select as well between polysilicon and PSG. Since the HF-PSG etch front moves laterally, it takes very long etch times to produce long structures. To solve this problem, one must put etchant access holes in the polysilicon structure, which effectively increases etch-front area and keeps the etch time manageably small (Fig. 5).

Stiction. A problem that has plagued micromachinists is the so-called stiction between released polysilicon structures and the underlying silicon substrate. After the sacrificial layer is etched away, the wafers are usually cleaned in successive baths of water. Then, in the wafer drying process, the water–air interface eventually contacts both the polysilicon and the underlying silicon. Surface tension pulls the polysilicon and silicon into contact. The surfaces may then stick together permanently because of van der Waals forces or polymeric residue from the earlier use of photoresist. Solutions to the stiction problem include drying with supercritical carbon dioxide and sublimation of solid carbon dioxide (dry ice). The use of certain organic self-assembled monolayers can reduce the incidence of stiction occurring during device operation. Use of surface area reducing dimples are also used as shown in Fig. 5.

ACOUSTIC SENSORS AND ACTUATORS

Many sensing and actuation mechanisms employed in micromachined devices can be used in acoustic and ultrasonic devices. The frequency, power requirements, and signal-to-noise ratio often determine the choice of actuation mechanism.

Doped Silicon Strain Gauges

Strain-sensitive elements can be formed by doping single crystal silicon or polysilicon structures. Doped silicon elements have high-gauge factors and hence make good strain gauges. They can be used to measure strains caused by acoustic pressure in a gas or strain waves propagating in a solid structure. The piezoresistors are formed on the edges of the silicon diaphragm, where the maximum strain occurs in deflection (Fig. 6). Such strain gauges are always frequency limited. The resistance always has some capacitance (parasitic or intentional) in parallel with it that limits the bandwidth of this sensing method (7). For actuation, one can employ thermal expansion of multilayer structures that contain doped silicon.

Capacitive Elements

Diaphragm capacitors in micromachined structures can be formed readily by micromachining. Relatively large structures are used, so that their capacitances are much bigger than the parasitic capacitance of their electrical interconnecting leads.

For sensing, the incoming pressure or stress waves change the capacitor gap and the capacitance. This change in capacitance can be measured using a charge sensitive op-amp. For actuation, the gap can be modulated by applying an ac voltage on the capacitor. The resultant diaphragm movement pushes fluids and hence launches acoustic waves. An example of such a device is the MUT (micromachined ultrasonic transducer) device (Fig. 7) developed at Stanford University (16).

Piezoelectrics

The piezoelectric effect is a result of the nonsymmetrical distribution of ions in the basic unit cell of certain crystals, such as quartz. The nonsymmetrical charge results in a net dipole moment when the unit cell is compressed or expanded. When integrated through the piezoelectric volume, this dipole moment results in a net charge on the surfaces. The application of a stress on a piezoelectric material results in a net polarization charge. This is known as the direct piezoelectric effect. The converse piezoelectric effect is characterized by the generation of stress and strain in a piezoelectric solid upon the application of an electric field. The applied electric field causes a net force on the nonuniform charge density in each unit cell. This force causes the ionic charge centers to

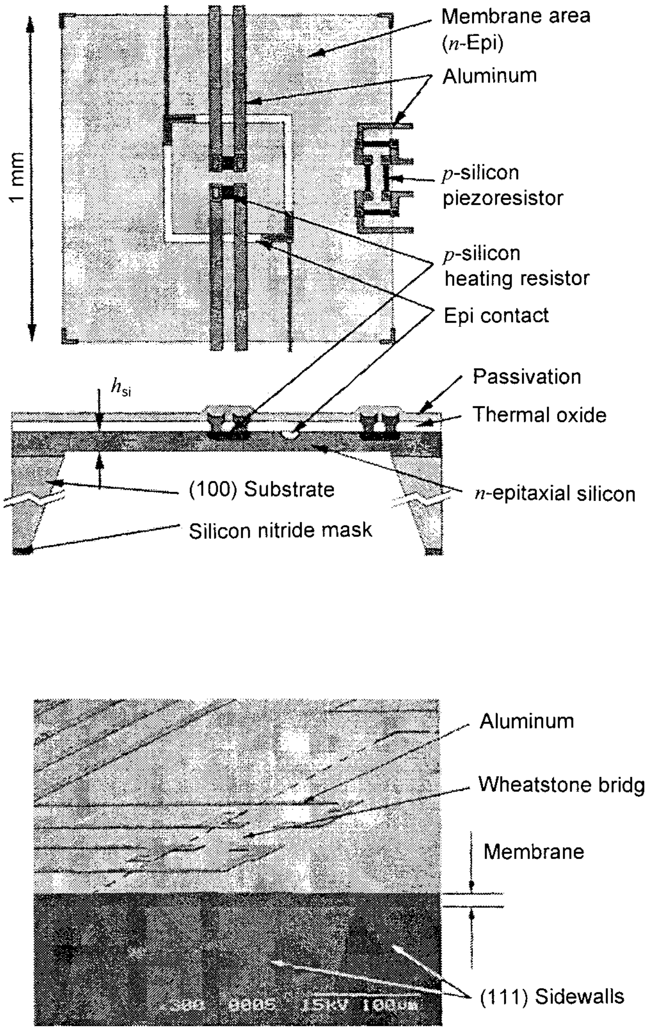

Figure 6. Micromachined thermally actuated resonator. Top: Top view of die showing piezoresistors for actuation (heating) and sensing (piezoresistor). Middle: Cross-section view. Bottom: Scanning electron microscope (SEM) of die.

move, and this causes net extension or contraction of the unit cell.

In micromachined devices one generally does not use piezoelectric crystals but rather thin films made of small piezoelectric crystal grains. Thin films of piezoelectric ZnO, AlN, and PZT (lead zirconate titanate) have the common feature of containing microscopic grains of crystals. If these grains were randomly oriented, the net piezoelectric effect from the grains would cancel out. However, the thin films are often deposited so that growth with oriented grains occurs. For ferroelectric films like PZT, the unit cells are oriented by electrical poling methods. A more detailed discussion of piezoelectric thin films is given in THIN FILMS.

Piezoelectric films have been used widely as acoustic and ultrasonic sensing elements. The main advantages to using piezoelectric thin films are high electromechanical coupling and very high bandwidths. Piezoelectric devices have been used to sense ultrasonic waves at frequencies up to the GHz range.

Flexural Plate Wave Device. The flexural plate wave device (FPW) was developed at Berkeley (8). Thin film ZnO interdigitated fingers are used to excite alternating contraction and expansion zones on a micromachined silicon nitride membrane (see Fig. 8). When driven at high frequencies, these transducers launch flexural plate waves along the micromachined thin diaphragm. An intriguing feature of FPWs is that their phase velocity is a linear function of the plate thickness for very small plate-to-wavelength ratios. Micromachining allows these plates to be made a few microns thick. Wavelengths are typically 100 μm. With such numbers, the phase velocity is 300 m/s to 500 m/s. This is much lower than the velocity of sound in most liquids and gases. The speed difference results in evanescent waves instead of propagating waves to be produced near the vibrating membrane. Most of the wave energy is trapped near the membrane and is not dissipated. This is similar to the light-trapping property of fiber optic cables, where the speed of light in the core of the fiber is lower than that in the surrounding cladding material. The ultrasonic flexural plate waves have been used as very sensitive gas and liquid sensors.

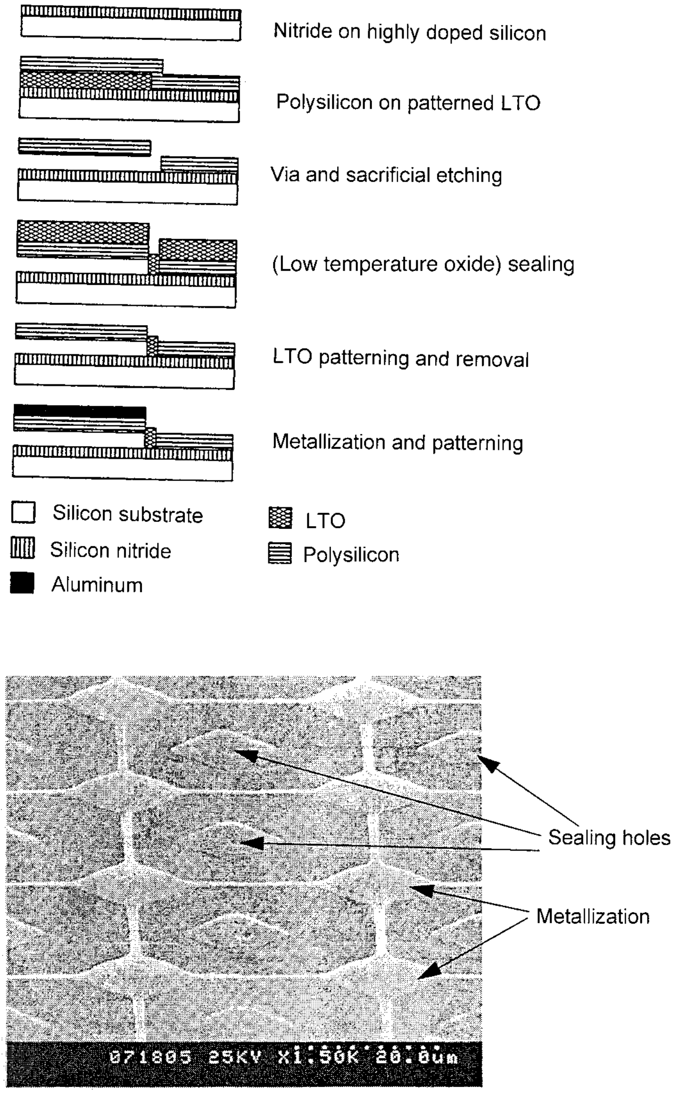

Figure 7. Surface micromachined ultrasonic transducers. Top: Fabrication process with cavity sealing. Bottom: SEM of diaphragms with sealing holes.

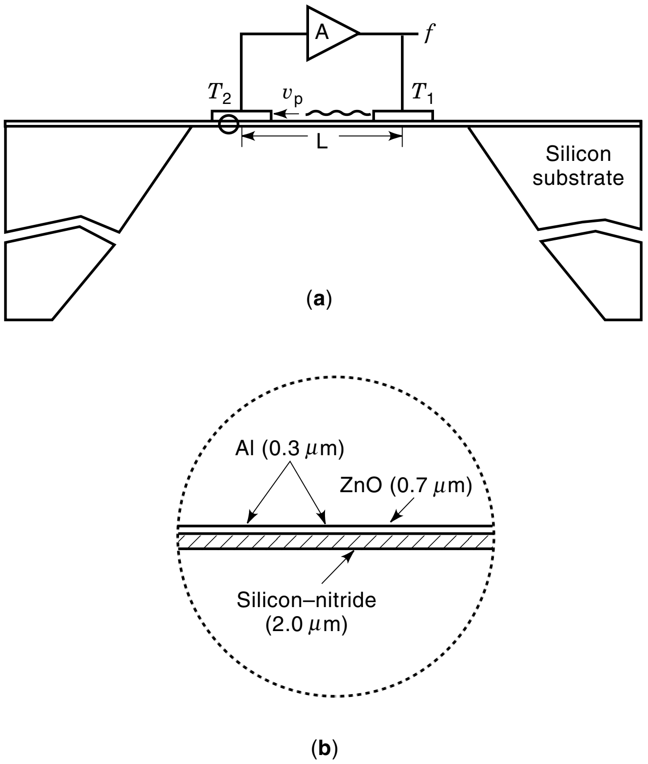

(a)

(b)

Figure 8. Flexural plate wave device showing interdigitated aluminum electrodes.

Microphone. The bimorph structure has been used for microphone applications, as shown in Fig. 7 (9). The process flow diagram displays the bulk-micromachining process used to create the piezoelectric structure. The impinging sound waves bend the cantilever beam, causing the ZnO thin film to generate a voltage that can be measured.

Ultrasonic Micromotor. Seen in Fig. 8 is a micromachined micromotor made with thin-film PZT (10). The PZT film was deposited on the silicon nitride membrane using the sol-gel method. The rotor was positioned to make frictional contact with the membrane so that, when the membrane vibrated at one of its transverse modes, the rotor moved.

ACOUSTIC DEVICE MODELING

Acoustic sensors are used for detecting mechanical pressure and velocity waves in fluids, and stress and particle velocities in solids. Correspondingly, acoustic actuators generate mechanical waves in fluids and solids. The generation and sensing is generally done electrically because of the availability of high-quality efficient electrical sources, amplifiers and filters. Hence, at the heart of any acoustic device are electric and mechanical components. An important figure of merit for acoustic transducers therefore becomes the efficiency with which electrical energy and mechanical energy are converted into each other. This efficiency is often defined as the ratio of the mechanical energy stored to the electrical energy stored in the device.

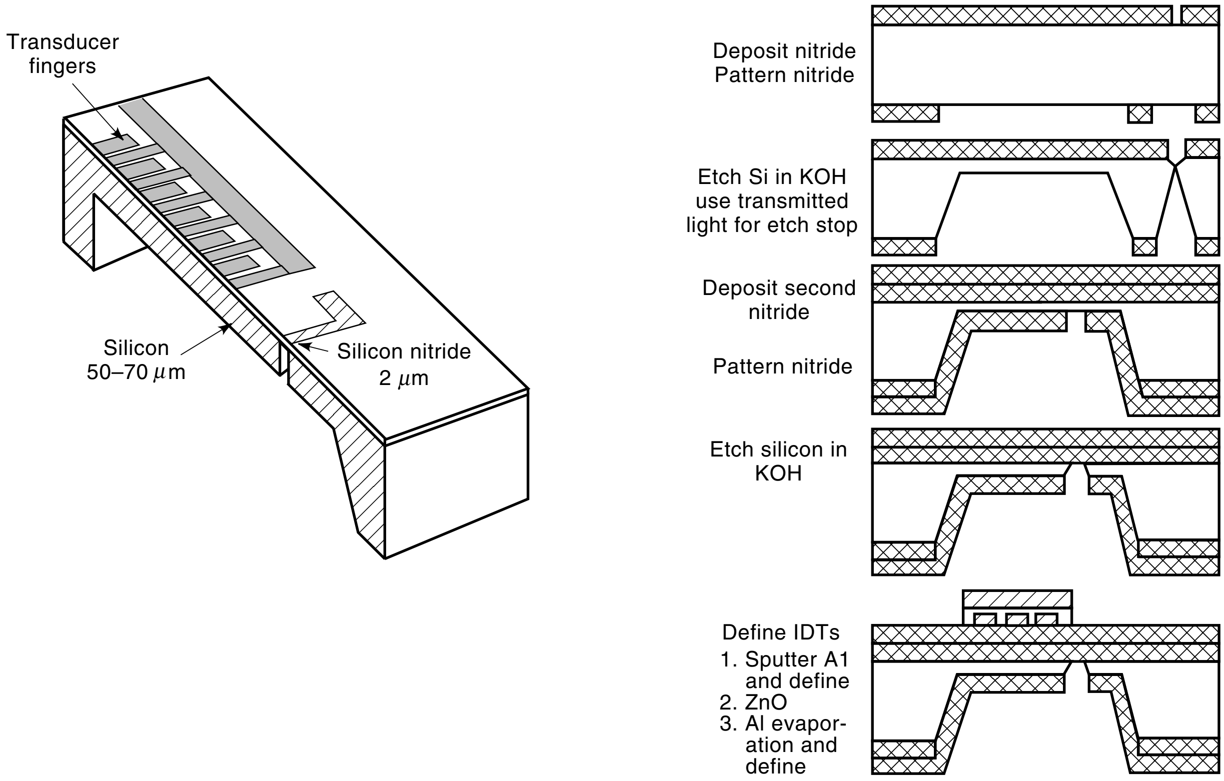

Figure 9. Cross-section of a piezoelectric device used as a microphone and microspeaker. The process used to fabricate the device is shown on the right.

Before discussing efficiency issues, we have to consider device models. In addition to analytical and physical modeling, a large effort in numerical modeling using finite element methods is being made for MEMS devices. Thermal, fluid, and electromagnetic effects can be strongly coupled in any real MEMS system, and so analytical modeling becomes nearly impossible. Furthermore very small features connected to much larger substrates require novel ways of modeling. In response to this need, new companies are focusing on MEMS finite element simulation. Examples are MEMCAD, Tanner Research, and Coyote Systems. Several academic groups are also developing CAD for MEMS, an example being SUGAR, which is being developed at Berkeley.

There are two regimes of acoustic device operation to be distinguished by the wavelength-to-device-dimension ratio. If the acoustic wavelength is much bigger than the device, the device can be thought of as a point source or a receiver, wave effects can be ignored, and lumped element models can be used. If the acoustic wavelength at the operating frequency is much smaller than the device dimensions, one has to consider wave phenomena in the device because multiple wavelengths can fit in the device.

Lumped Element Models (Wavelength $\gg$ Device Dimensions)

In this regime, the mechanical parts of acoustic devices, which are diaphragms, beams, or plates, all move nearly in phase throughout the entire device. Therefore the mechanical parts can be represented as discrete mass-spring systems. Furthermore, the mass-spring systems can be modeled as equivalent electrical circuits by making analogies between the mechanical and electrical variables. For example, one possible analogy is to model forces as voltages and velocities as currents. Using this analogy, discrete masses can be modeled as inductors, and discrete springs can be modeled as capacitors. An equivalent electrical resistor can model the lossy viscous effects in mechanical parts. The coupling of the real electrical circuit to the equivalent electrical model of the mechanical device is obtained through an equivalent transformer whose transformer ratio is related to the electromechanical coupling constant defined above. This simplified model is often very useful for device characterization and optimization. An example of such a system is the microphone and the bimorph described below.

Continuous-Wave Models (Wavelength $<$ Device Dimensions)

In this regime, the parts of an acoustic device can move with different phases. This leads to wave phenomena inside the device. The device behavior is characterized by differential equations that have certain eigenfunctions as solutions. Superposing the eigenfunctions yields the mechanical disturbances on the device. Even though a discrete model that is good for all the modes is not possible, any given eigenfunction can be equated to an equivalent spring-mass-damper. This mechanical system can then again be equated to an electrical circuit.

An example is the modeling of the fundamental mode of the longitudinal mode resonant transducer (LMRT) shown in Fig. 9. The metal version of the transducer consists of a back and a front side, between which a piezoelectric ceramic such as PZT is held in compression. When the PZT is driven at the longitudinal mode resonance frequency of the structure, large motions at the horn side can be achieved. Such transducers are used to generate high-amplitude ultrasound. The limitations of these devices are the material properties of the toughest metals (titanium alloys) and the PZT bonding efficiency. The alternative silicon-micromachined version of such a

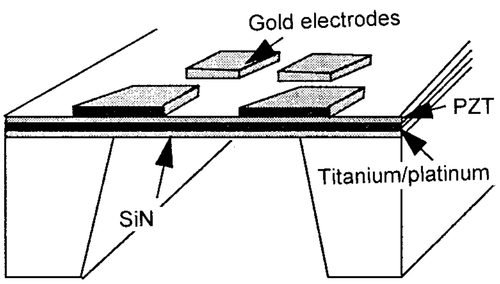

Schematic of the micromachined thin-film PZT/metal sandwich transducer

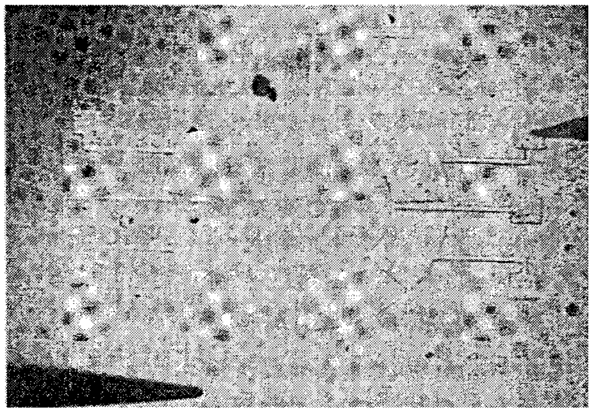

Eight-pole stator has an inner diameter of 1.2 mm and outer diameter of 2 mm, placed on a 2.2 mm × 2.2 mm membrane. Extra 4 pads for sensing are also provided.

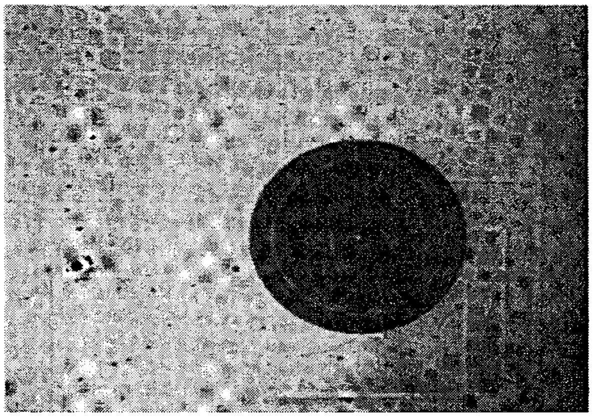

A plano-convex 1.5 mm diameter lens is placed convex surface down. The lens spins at 100 to 300 rpm.

Figure 10. Piezoelectrically activated micromotor.

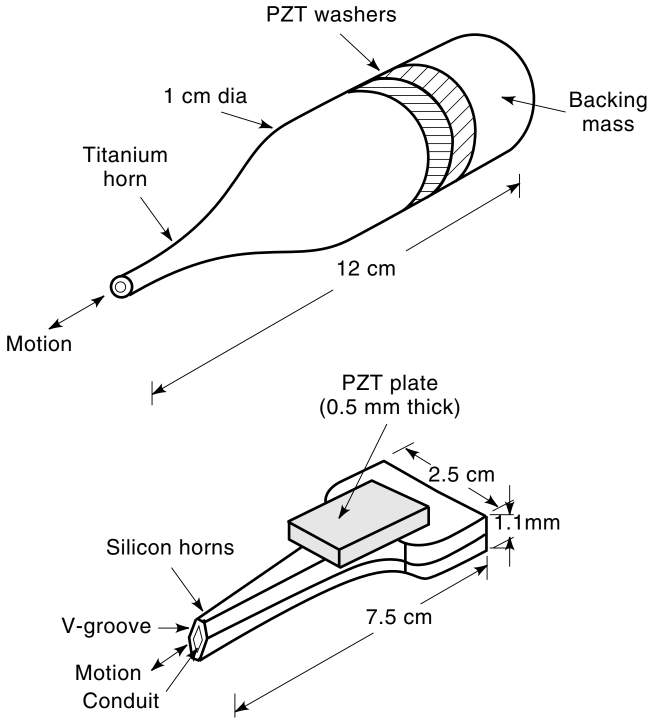

Figure 11. Longitudinal mode resonators. Top: Metal alloy/PZT high-intensity transducer. Bottom: Corresponding micromachined silicon/PZT transducer.

transducer is the horn at the bottom of the figure (11,12). These transducers have been used to cut tissue, pump liquids, and atomize liquids. Because of the silicon material properties mentioned above, displacements as large as those produced by the metal transducers can be generated with much smaller transducers.

Acoustic Pumping and Fluid Models

The interaction of fluids with a vibrating surface is important in acoustic devices. Acoustic waves generated by actuators travel through various media and get received at sensing devices. Classical acoustics has been developed very far and many analytical solutions to fluid coupling are available in texts. A very interesting MEMS application of acoustic-fluid interaction is the flexural plate wave pump that utilizes acoustic streaming (13). Another example of acoustic force utilizing micromachined device is shown in Fig. 10. Here the ultrasound generated by a thin film ZnO actuator is focused at the fluid-air interface where nonlinear acoustic forces can cause ejection of liquid droplets (14).

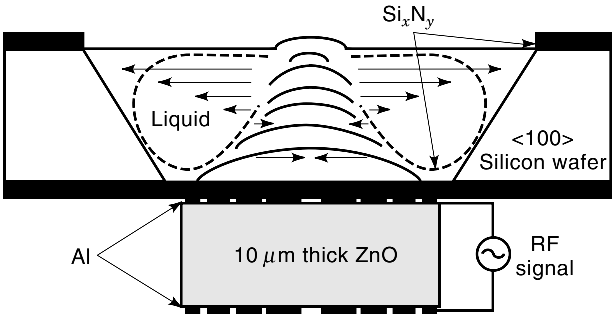

Figure 12. Micromachined liquid mixer and ejector.

SUMMARY

Micromachining techniques have been used to make acoustically relevant mechanical and actuating structures. Micromachining allows the fabrication of structures that are in the micron size domain. Membranes, cantilevers, and beams can be made that have the same acoustic response as larger structures by making their lateral dimensions smaller and keeping plate stiffnesses the same by reducing plate thickness. This recipe allows miniaturization of acoustic and ultrasonic devices.

In addition to the new domain of physical size for acoustic devices, micromachining in silicon makes available unique material properties that cannot be found in conventional metal-based transducers. Silicon is very strong and can be driven to much higher amplitudes than the metal counterparts. Silicon's high thermal conductivity and small acoustic losses permit one to make very high-quality and resilient acoustic actuators and sensors.

The further capability to integrate solid-state sensors and electronic circuits into the acoustic structure enables one to realize large improvements in signal-to-noise and system performance. Parasitic capacitances and resistive lead losses in sensitive sensors can be minimized. Integration of electronics reduces system size and complexity. Arrays of inexpensive devices can be fabricated for faster signal processing.

As micromachining becomes more widespread, acoustic devices made using the technology will become more common. Most of the work thus far has been conducted in university laboratories, but more recently, industry is starting to investigate and make micromachined acoustic devices (15). In the future, as the integration of micromechanical and electronic elements proceeds, one can expect to see an increasing number and variety of micromachined ultrasonic and acoustic devices become available (16).

BIBLIOGRAPHY

1. K. S. Suslick, *Ultrasound: Its Chemical, Physical, and Biological Effects,* New York: VCH, 1988.
2. E. A. Yasumura, A study of microcantilever quality factor, presented at *Solid State Sensor and Actuator Workshop,* Hilton Head, SC, 1998.
3. A. Lal and R. M. White, Silicon microfabricated horns for power ultrasonics, *Sensors and Actuators,* **54**: 542–546, 1996.
4. M. Madou, *Fundamentals of Microfabrication,* Boca Raton, FL: CRC Press, 1997.
5. P. Rai-Choudhary, *Handbook of Microlithography, Micromachining, and Microfabrication,* Vol. 2, Bellingham, WA: SPIE, 1997.
6. S. D. Collins, Etch stop techniques for micromachining, *J. Electrochem. Soc.,* **144**: 2242, 1997.
7. E. A. Sheplak, A wafer-bonded, silicon-nitride membrane microphone with dielectrically isolated, single-crystal silicon piezoresistors, presented at Solid State Sensor and Actuator Workshop, Hilton Head, SC, 1998.
8. S. W. Wenzel, B. A. Martin, and R. M. White, Generalized lamb-wave multisensor, presented at *Proc. IEEE Ultrasonics Symp.,* Chicago, IL, 1988, pp. 735–743.

9. A. Lal and R. M. White, Micro-fabricated acoustic and ultrasonic source-receiver, presented at *Transducers' 93,* Yokohama, Japan, 1993.
10. A. M. Flynn et al., Piezoelectric micromotors for microrobots, *J. Microelectromech. Devices,* **1**: 44, 1992.
11. A. Lal and R M. White, Silicon micro-fabricated horns for power ultrasonics, presented at *Transducers' 95,* Stockholm, Sweden, 1995.
12. A. Lal and R. M. White, Micromachined silicon ultrasonic atomizer, presented at *IEEE Ultrasonic Symp.,* San Antonio, TX, 1996.
13. R. M. Moroney, R. M. White, and R. T. Howe, Ultrasonic micromotors: Physics and applications, presented at *IEEE Micro Electro Mech. Syst.,* 1990.
14. X. Zhu and E. S. Kim, Acoustic-wave liquid mixer, presented at *Microelectromechanical System (MEMS) ASME International Congress,* Dallas, TX, 1997.
15. P. R. Schreeper et al., A review of silicon microphones, *Sensors and Actuators,* **44**: 1, 1994.
16. X. C. Jin et al., Surface micromachined capacitive ultrasonic immersion transducers, presented at *IEEE MEMS 98,* Heidelberg, Germany, p. 649.

AMIT LAL
University of Wisconsin, Madison
RICHARD M. WHITE
University of California, Berkeley

ULTRASONIC APPLICATIONS. See SEMICONDUCTOR ULTRASOUND TREATMENT.